



Critical behaviour study of ferroelectric semiconductors $(\text{Pb}_x\text{Sn}_{1-x})_2\text{P}_2\text{S}_6$ from thermal diffusivity measurements

V. Shvalya ^{a,b}, A. Oleaga ^{a,*}, A. Salazar ^a, A.A. Kohutych ^b, Yu.M. Vysochanskii ^b

^a Departamento de Física Aplicada I, Escuela Técnica Superior de Ingeniería, Universidad del País Vasco, Alameda Urquijo s/n, 48013 Bilbao, Spain

^b Institute for Solid State Physics and Chemistry, Uzhgorod University, 88000 Uzhgorod, Ukraine



ARTICLE INFO

Article history:

Received 19 May 2015

Received in revised form 23 August 2015

Accepted 25 August 2015

Available online 29 August 2015

ABSTRACT

An ac photopyroelectric calorimeter has been used to study the thermal diffusivity of the ferroelectric semiconductors family $(\text{Pb}_x\text{Sn}_{1-x})_2\text{P}_2\text{S}_6$ ($x = 0.1$ to 1) from low temperature to room temperature. A typical behaviour of poor thermal conduction has been observed, ascertaining the role of phonons as heat carriers. The substitution of Sn by Pb leads to an increase in thermal conduction due to the different ionic size. Thermal anisotropy has been found in this monoclinic structure, with heat diffusion being easier in the $(1\ 0\ 0)$ direction. The second order character of the paraelectric to ferroelectric transition has been checked and a crossover in the evolution of its critical behaviour has been found, from a clear non-mean field model at $x = 0.1$ (where a model including both first-order fluctuations as well as the presence of defects needs to be considered) to a mean field one at $x = 0.3$. Besides, phenomenological parameters in the Landau expansion applied to the ferroelectric phase have given values in agreement with literature.

© 2015 Elsevier B.V. All rights reserved.

1. Introduction

$\text{Sn}_2\text{P}_2(\text{S}_{1-x}\text{Se}_x)_6$, $(\text{Pb}_x\text{Sn}_{1-x})_2\text{P}_2\text{S}_6$, $(\text{Pb}_x\text{Sn}_{1-x})\text{P}_2\text{Se}_6$ are a broad family of ferroelectric semiconductors specially interesting both from a practical aspect (they present promising photorefractive, acoustooptics, and electrooptics properties [1,2]) and from the solid state physics point of view as their phase diagram is quite complex, with the presence of a Lifshitz point, incommensurate phases, first and second order phase transitions (see Fig. 1) [3]. The detailed measurement of certain thermal properties, such as specific heat, in the near vicinity of the ferroelectric phase transition can give us information about the physical mechanisms playing a relevant role at the transition, as stated by the theory of critical behaviour. After this theory, specific heat must fulfil the following equation near the critical temperature T_C , written as a function of the reduced temperature $t = (T - T_C)/T_C$ in the case of second order phase transitions:

$$c_p(T) \sim |t|^{-\alpha} \quad (1)$$

where α is called the critical exponent. Renormalization group theory has predicted different “universality classes” with different values of α as a function of the mechanisms required to correctly describe the Hamiltonian of the system in the near vicinity of T_C . For simple uniaxial ferroelectrics, the ferroelectric phase is well

described by the Landau classical model while the paraelectric phase falls within the category of the “mean field model” ($\alpha = 0$, long-range order interactions are the main drivers of the transition), or very close to it, with the introduction of a small logarithmic correction [4,5]. But it will separate from the mean field model (and thus α will be different from 0) if fluctuations of the order parameter are important or some other mechanisms are present. In particular, Lifshitz terms as well as uniaxial dipolar interactions have been theoretically proposed to describe the critical behaviour of $\text{Sn}_2\text{P}_2(\text{S}_{1-x}\text{Se}_x)_6$ (see the review by Folk and Moser [6] and references therein) which have been put to test by different experimental works [7–14]. In particular, Oleaga et al. [14] have published the evolution of this critical behaviour from $x = 0$ to $x = 0.30$ past the Lifshitz point ($x = 0.28$), showing that in the concentration region near the Lifshitz point the Lifshitz universality class L describes better the situation than classes which takes into account tricriticality or strong long-range dipolar interactions. Renormalization group theory states that the presence of a Lifshitz point enhances the fluctuations in the order parameter deviating the critical exponents from the typical mean-field values ($\alpha = 0$) to $\alpha = 1/4$ in systems with short range interactions [15]. On the other hand, in order to describe the critical behaviour of $\text{Sn}_2\text{P}_2\text{S}_6$ ($x = 0$), a model taking into account both fluctuations of the order parameter and the presence of defects was needed [11]. The aim of this work is to study the critical behaviour of $(\text{Pb}_x\text{Sn}_{1-x})_2\text{P}_2\text{S}_6$, ($0.1 \leq x \leq 1$) and compare it to the already known of $\text{Sn}_2\text{P}_2(\text{S}_{1-x}\text{Se}_x)_6$. The phase diagram is much simpler in this case as there is neither a Lifshitz point, nor an

* Corresponding author.

E-mail address: alberto.oleaga@ehu.es (A. Oleaga).

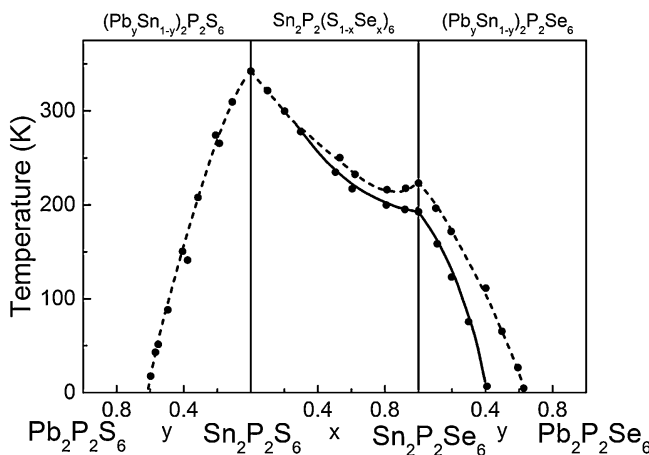


Fig. 1. Phase diagram of $\text{Sn}_2\text{P}_2(\text{S}_{1-x}\text{Se}_x)_6$, $(\text{Pb}_y\text{Sn}_{1-y})_2\text{P}_2\text{S}_6$, $(\text{Pb}_y\text{Sn}_{1-y})_2\text{P}_2\text{Se}_6$. The dashed lines indicate the second-order phase transitions from the paraelectric phase to the ferroelectric one in $(\text{Pb}_y\text{Sn}_{1-y})_2\text{P}_2\text{S}_6$ and to incommensurate phase in $\text{Sn}_2\text{P}_2(\text{S}_{1-x}\text{Se}_x)_6$ and $(\text{Pb}_y\text{Sn}_{1-y})_2\text{P}_2\text{Se}_6$. The continuous lines indicate the first order transition from the incommensurate to the ferroelectric phase.

incommensurate intermediate phase at certain concentrations but simply a paraelectric to ferroelectric phase transition up to $x=0.6$ (see Fig. 1) [3,16].

In order to carry out this kind of study, suitable techniques must be employed. The ac photopyroelectric calorimetry is a technique particularly fitted to study the critical behaviour of phase transitions as a small temperature gradient in the sample gives rise to a high signal-to-noise ratio in the detector, so the features of the transition in the near vicinity of the critical temperature can be studied with great detail. The usefulness of this technique has been well demonstrated in the study of the critical behaviour of a variety of second-order phase transitions in a wide range of materials, measuring either specific heat (c_p) or thermal diffusivity (D) [17–22]; see the paper by Zammit et al. [23] for an in-depth review of its applications.

2. Samples and experimental techniques

Single crystals of $(\text{Pb}_x\text{Sn}_{1-x})_2\text{P}_2\text{S}_6$ were obtained by the vapor-transport method ($x=0, 0.10, 0.20, 0.30, 0.45, 0.80$ and 1) in a quartz tube using SnI_2 as a transport agent. The synthesis of the starting material in the polycrystalline form was carried out using high-purity elements Sn (99.99%), Pb (99.99%), P (99.999%), S (99.99%) in atomic percentage. The $\text{Sn}_2\text{P}_2\text{S}_6$ and $\text{Pb}_2\text{P}_2\text{S}_6$ single crystals were also grown by crystallization from melt using the Bridgman method. For vapor-transport grown samples the chemical content could be nonstoichiometric. There is no corroboration about the agreement of the nominal stoichiometry and the one in the so obtained samples. However, as was confirmed by XPS spectroscopy of $\text{Sn}_2\text{P}_2\text{S}_6$ crystals the atomic concentration of Sn could be up to 2% higher than the nominal value [24]. For the mixed crystals grown by vapor transport, it has been found by means of atomic absorption spectroscopy that the contents of Sn and Pb can deviate from the nominal value in less than 0.2% [25].

It is already well established that the crystalline structure is monoclinic with point group $2/m$ for the paraelectric phase while it is m for the ferroelectric one [3]. Thin slabs (with thicknesses in the range 300–500 μm) with their faces in the monoclinic symmetry plane perpendicular to $(0\ 1\ 0)$ direction were prepared for thermal diffusivity measurements. In the case of $\text{Pb}_2\text{P}_2\text{S}_6$ two additional samples with faces perpendicular to $(1\ 0\ 0)$ and $(0\ 0\ 1)$ directions where also cut in order to check the possible thermal anisotropy, as has already been shown for $\text{Sn}_2\text{P}_2\text{S}_6$ [11]. Thermal diffusivity

measurements have been performed by a high-resolution ac photopyroelectric calorimeter in the standard back detection configuration [26,27], obtaining D in the direction perpendicular to the plane parallel faces in each case. A modulated low power diode laser beam illuminates the front surface of the sample, whose rear surface is in thermal contact with a LiTaO_3 pyroelectric detector with metallic electrodes on both faces, by using an extremely thin layer of heat-conductive silicone grease. The samples have been covered with a very thin layer of graphite to make them opaque, which is a customary procedure. The photopyroelectric signal is processed by a lock-in amplifier in the current mode. Both sample and detector are placed inside a closed cycle helium cryostat that allows measurements in the temperature range from 18 K to room temperature, at heating/cooling rates that vary from 100 mK/min for measurements on a wide temperature range to 10 mK/min for high-resolution runs close to the phase transitions to study their critical behaviour.

If the sample is opaque and thermally thick (i.e. its thickness ℓ is higher than the thermal diffusion length $\mu = \sqrt{D/\pi f}$, f being the modulation frequency) the natural logarithm of the amplitude and the phase of the normalized photopyroelectric current at a fixed temperature have a linear dependence on \sqrt{f} , with the same slope m , from which the thermal diffusivity of the sample can be measured [27,28]:

$$D = \frac{\ell^2 \pi}{m^2} \quad (2)$$

Once the thermal diffusivity has been measured at a certain reference temperature (D_{ref}), the temperature is changed while recording the phase of the photopyroelectric signal. Defining that phase difference with temperature as $\Delta\Psi(T)$, the temperature dependence of the thermal diffusivity is given by [29]:

$$D(T) = \left[\frac{1}{\sqrt{D_{ref}}} - \frac{\Delta\Psi(T)}{\ell \sqrt{\pi f}} \right]^{-2} \quad (3)$$

It is worth noting that this measurement is performed varying the temperature continuously and not just taking values of D at certain temperatures and that data are retrieved every several seconds. Depending on the rate of the heating/cooling run, the total number of points in a curve varies but in a typical curve there are several thousands of experimental points, with a resolution of 0.01 K in temperature. This is what allows retrieving the precise shape of the thermal diffusivity as a function of temperature.

The modulation frequencies used for this study have been in the range (1–21 Hz) depending on the thickness of the particular sample and the temperature range of the measurements, always ensuring that we are working in the linear region where Eq. (2) is fulfilled.

In order to study the critical behaviour of the transition, very well defined thermal diffusivity curves have been obtained in the near vicinity of the critical temperatures. As thermal diffusivity is inversely proportional to specific heat c_p through

$$D = \frac{K}{\rho c_p}, \quad (4)$$

where K is the thermal conductivity and ρ the density, the critical behaviour of specific heat and the inverse of thermal diffusivity is the same, provided that neither thermal conductivity nor density have significant changes at the transition, which is the case in these materials [11,30].

3. Experimental results

In the first place, thermal diffusivity was measured at room temperature ($T=292$ K) for all concentrations in the $(0\ 1\ 0)$ direction in

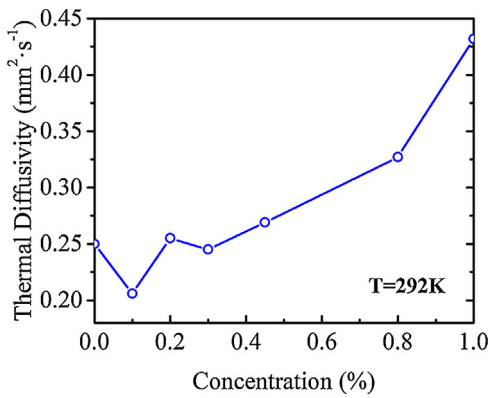


Fig. 2. Thermal diffusivity as a function of lead concentration for the family $(\text{Pb}_x\text{Sn}_{1-x})_2\text{P}_2\text{S}_6$ at $T = 292 \text{ K}$.

order to better compare them. Fig. 2 shows their values (between 0.206 and $0.432 \text{ mm}^2/\text{s}$) which are within a typical range for poor thermal conductors, where heat is mainly transferred by phonons. Slightly substituting Sn by Pb reduces D a little bit while further doping steadily increases it till a value of $0.42 \text{ mm}^2/\text{s}$ is reached for $\text{Pb}_2\text{P}_2\text{S}_6$ ($x = 1$). The size of the ionic radius of Pb^{2+} is larger than that of Sn^{2+} , and so the addition of lead increases the space available for Sn^{2+} in mixed single crystals [3,16]. This situation might reduce the phonon scattering process and therefore the phonon mean free path would be increased.

Fig. 3 shows the evolution of D with temperature from room temperature down to 60 K obtained as a continuous measurement

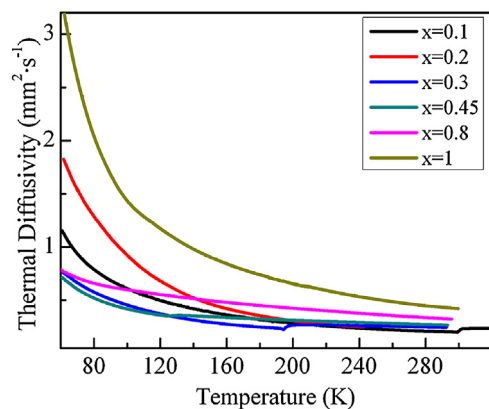


Fig. 3. Thermal diffusivity as a function of temperature for the family $(\text{Pb}_x\text{Sn}_{1-x})_2\text{P}_2\text{S}_6$.

as explained in Section 2. Each curve has several thousands of experimental points, that's why it seems as if it were a continuous line. The thermal diffusivities measured at 292 K were taken as a reference for each curve. The general trend is an increase as temperature is reduced; in thermal insulators, heat is transferred by phonons and their mean free path is quickly increased as temperature decreases. In four curves ($x = 0.1, 0.2, 0.3, 0.45$) there is a dip superimposed on the general increase of D , signalling the presence of the paraelectric to ferroelectric transition; as they are not well discerned in Fig. 3, Fig. 4 shows them in detail. In all cases, the possible thermal hysteresis of the transition has been checked and

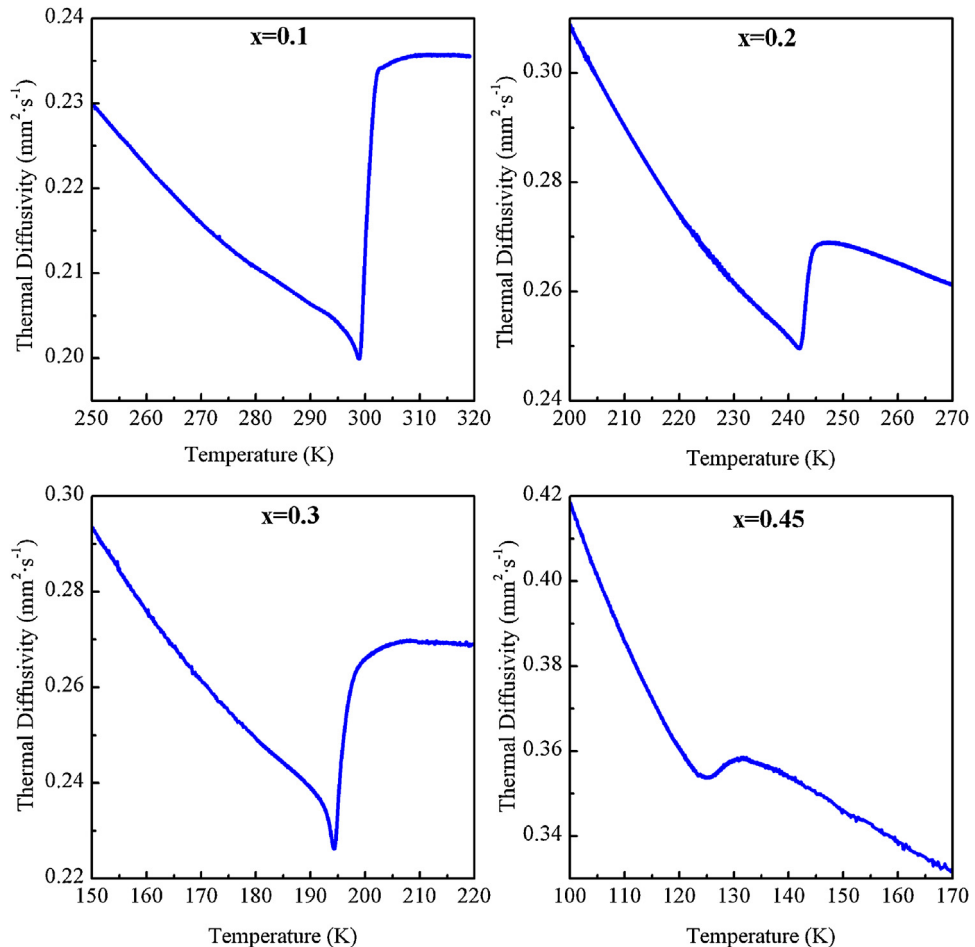


Fig. 4. Detail of the thermal diffusivity curves for $(\text{Pb}_x\text{Sn}_{1-x})_2\text{P}_2\text{S}_6$ ($x = 0.1, 0.2, 0.3, 0.45$) around the paraelectric to ferroelectric transition in each case.

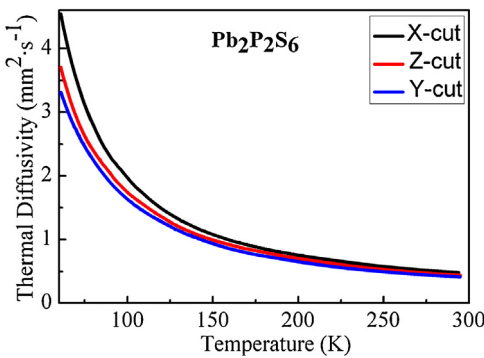


Fig. 5. Thermal diffusivity as a function of temperature for $\text{Pb}_2\text{P}_2\text{S}_6$ samples with faces perpendicular to (1 0 0) (X-cut), (0 1 0) (Y-cut), and (0 0 1) (Z-cut).

in all of them it has been confirmed that there is no difference in cooling or heating runs by using slow enough temperature rates (as low as 20 mK/min), thus confirming the second order character of this ferroelectric transition. The critical temperature of the transition is reduced as lead concentration is increased, since Sn^{2+} ions can move with smaller thermal energy as the space available for them is increased [16]. Lastly, in the case of $x=0.8$ and 1, measurements have been performed down to 18 K, confirming the absence of a phase transition.

Lastly, as these samples are monoclinic, thermal anisotropy can be expected. Indeed, in the case of $\text{Sn}_2\text{P}_2\text{S}_6$ ($x=0$) it is clearly established in literature that heat transfer is easier in the (1 0 0) direction and more difficult in the (0 1 0) one, while (0 0 1) gave D values in between [11]. This has been checked for the case of $\text{Pb}_2\text{P}_2\text{S}_6$ ($x=1$) and is presented in Fig. 5. The same sequence is found for $x=1$ as for $x=0$, confirming the thermal anisotropy of the family, where heat is more easily transferred along the X direction.

4. Critical behaviour and discussion

4.1. Landau model

As seen in Fig. 4, only the critical behaviour of three phase transitions can be studied ($x=0.1, 0.2, 0.3$). The dip for $x=0.45$ is too rounded to be useful to perform any quantitative treatment on it. This type of rounding is quite common in heavily doped systems: as Pb ions are introduced in the compound in a high percentage, the disorder and the defects increase noticeably smearing the shape of the phase transitions.

The first approach that we have taken is through the mean-field analysis in terms of Landau theory where we are taking into account the possible coupling of polarization to strain in a uniaxial ferroelectric and so Landau thermodynamical potential density reads:

$$F = F_0 + \frac{\alpha t}{2} P^2 + \frac{\beta}{2} P^4 + \frac{\gamma}{2} P^6 + \frac{1}{2} c u^2 + r u P^2 \quad (5)$$

where F_0 is the value in the paraelectric phase, α is related to the Curie–Weiss constant, $t=T-T_C$ with T_C the transition temperature, β and γ are phenomenological coefficients which don't depend on temperature, $c=c_{ijkl}$ is the elastic module matrix, $u=u_{ij}$ is the deformation tensor and $r=r_{ijkl}$ is the electrostriction coefficient [31].

The specific heat in the ferroelectric phase can be obtained by

$$c_p = -T \left(\frac{\partial^2 F}{\partial T^2} \right)_P \quad (6)$$

And taking into account Eq. (3), the anomalous part of the inverse of thermal diffusivity due to the transition reads, after Ref. [11]

$$\Delta \left(\frac{1}{D} \right) = p_1 \frac{T}{\sqrt{1 - 4p_2(T - T_C)}} \quad (7)$$

where $p_1 = a^2/(2\beta' K)$, $p_2 = \gamma a/\beta'^2$, $\beta' = \beta - 2r/c^2$.

In order to fit the inverse of thermal diffusivity, the full fitting equation has thus been

$$\frac{1}{D} = p_3 + p_4(T - T_C) + p_1 \frac{T}{\sqrt{1 - 4p_2(T - T_C)}} \quad (8)$$

where a linear term has been added to account for a regular contribution to the inverse of the thermal diffusivity as a function of temperature.

In Fig. 6 we can see the experimental results and the fittings for the three samples using Eq. (8), as well as the deviation plots (difference between the fitted values and the experimental ones divided by the experimental, in percentage); Table 1 contains the relevant parameters of the fitting, where the coefficient of determination R^2 expresses the quality of the fitting. They are quite good fittings so the values for the phenomenological coefficients β' and γ have been extracted from the fitted coefficients and are also included in that table. They fall within the range of already published values obtained by means of other techniques [32] which means that, indeed, the Landau model can explain the ferroelectric phases.

4.2. Renormalization group theory

Let's turn our attention to the paraelectric phase. If we are to apply renormalization group theory in its strictest sense, both branches of the transition (paraelectric as well as ferroelectric) should comply with the following equation

$$\frac{1}{D} = B_1 + C_1 t + A_1^\pm |t|^{-\alpha} (1 + E^\pm |t|^{0.5}) \quad (9)$$

where $t=(T-T_C)/T_C$ is the reduced temperature. Superscripts + and – stand for $T > T_C$ and $T < T_C$ respectively. The linear term represents the regular contribution to the inverse of the thermal diffusivity, while the last term represents the anomalous contribution at the second order phase transition. The factor under parenthesis is the correction to scaling that represents a singular contribution to the leading power as known from experiments and theory [17,33]. Scaling laws require that there is a unique critical exponent α for both branches and rigorous application states that constant B_1 needs also be the same [34]. These conditions have sometimes been relaxed in literature due to the difficulty of obtaining good fittings to the experimental data with those constraints, specially in the case of ferroelectrics. It is worth noting that in the previous work where $\text{Sn}_2\text{P}_2\text{S}_6$ ($x=0$) was studied, it was not possible to find a fitting under these strict conditions [11].

So, Eq. (9) has been applied to the three samples. The particular procedure followed for this kind of fittings is explained in full detail elsewhere [35]. In the case of $x=0.1$, the fitting was possible only accepting huge values of E^\pm , which perverts the meaning of the last correction term which must be, by definition, small, so this fitting was discarded. In the case of $x=0.2$ a fitting was found with a value of $\alpha=-0.07 \pm 0.02$ (approximating to zero, which would correspond to a mean field value) and acceptable values of the rest of the coefficients. For the case of $x=0.3$, the fitting was very good and $\alpha=-0.04 \pm 0.01$ (even closer to zero). The fittings for $x=0.2, 0.3$ are shown in Fig. 7, together with the corresponding deviation plots. Table 2 contains the relevant information about fitted parameters, temperature ranges used, quality of the fittings, etc. This behaviour

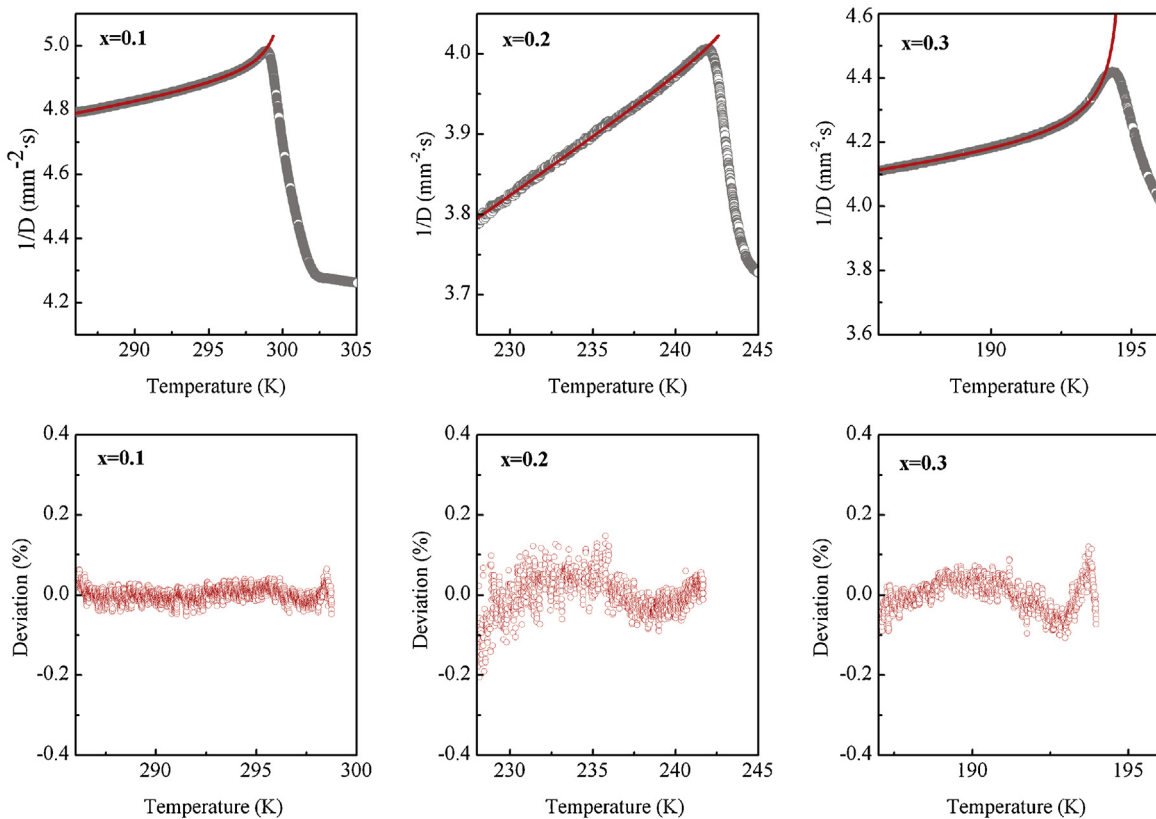


Fig. 6. ($\text{Pb}_x\text{Sn}_{1-x})_2\text{P}_2\text{S}_6$ ($x=0.1, 0.2, 0.3$). Above: Experimental data (circles) for the inverse of thermal diffusivity as a function of temperature. The lines represent the fits to Eq. (8) for the ferroelectric phase. Below: Deviation plots corresponding to the fits shown above.

Table 1

Results of the fitting of the inverse of thermal diffusivity using the Landau model (Eq. (8)). The columns show the adjustable parameters p_1 and p_2 , the fitted range in reduced temperature units $t=(T-T_C)/T_C$, the quality of the fitting through the coefficient of determination R^2 , as well as the calculated phenomenological parameters in the Landau expansion β' and γ .

	$x=0.1$	$x=0.2$	$x=0.3$
p_1 (s/mm^2)	$7.5 \times 10^{-4} \pm 8 \times 10^{-5}$	$1.26 \times 10^{-4} \pm 7 \times 10^{-6}$	$4.22 \times 10^{-3} \pm 1.6 \times 10^{-4}$
p_2 (K^{-1})	0.41 ± 0.06	0.16 ± 0.05	2.85 ± 0.28
Fitted range	4.4×10^{-2} – 2×10^{-3}	6×10^{-2} – 3.8×10^{-3}	4×10^{-2} – 3.2×10^{-3}
R^2	0.9997	0.9992	0.9993
$\beta'(\text{Jm}^5\text{C}^{-4})$	3.1×10^9	1.6×10^{10}	4.9×10^8
$\gamma(\text{Jm}^9\text{C}^{-6})$	1.6×10^{12}	2.5×10^{13}	4.25×10^{11}

Table 2

Results of the fitting of the inverse of thermal diffusivity using Eqs. (9), (10) and (12) for $x=0.1, 0.2$, and 0.3 , when a sensible fitting is found. In each case the relevant fitting parameters are shown together with the fitted range in reduced temperature units $t=(T-T_C)/T_C$ as well the quality of the fitting through the coefficient of determination R^2 .

	$x=0.1$	$x=0.2$	$x=0.3$
Eq. (9)	$A_1^+ (\text{s}/\text{mm}^2)$	0.76 ± 0.27	4.38 ± 0.81
	$A_1^- (\text{s}/\text{mm}^2)$	0.77 ± 0.28	4.32 ± 0.81
	α	-0.07 ± 0.02	-0.04 ± 0.01
	Fitted range for $T > T_C$	3.5×10^{-2} – 2.3×10^{-3}	5.3×10^{-2} – 2.7×10^{-3}
	Fitted range for $T < T_C$	6×10^{-2} – 3.8×10^{-3}	7.4×10^{-2} – 3.4×10^{-3}
Eq. (10)	R^2	0.997	0.999
	$A_2 (\text{s}/\text{mm}^2)$	0.014 ± 0.002	0.043 ± 0.005
	α	0.66 ± 0.02	0.369 ± 0.015
	Fitted range	3.2×10^{-2} – 2.7×10^{-3}	3.5×10^{-2} – 2.3×10^{-3}
Eq. (12)	R^2	0.979	0.986
	$A_4 (\text{s}/\text{mm}^2)$	$0.0292 \pm 7 \times 10^{-4}$	$-0.0119 \pm 2 \times 10^{-4}$
	$F_4 (\text{s}/\text{mm}^2)$	$7.06 \times 10^{-6} \pm 9.6 \times 10^{-7}$	$5.11 \times 10^{-6} \pm 2.5 \times 10^{-7}$
	Fitted range	3.2×10^{-2} – 2.7×10^{-3}	3.5×10^{-2} – 2.3×10^{-3}

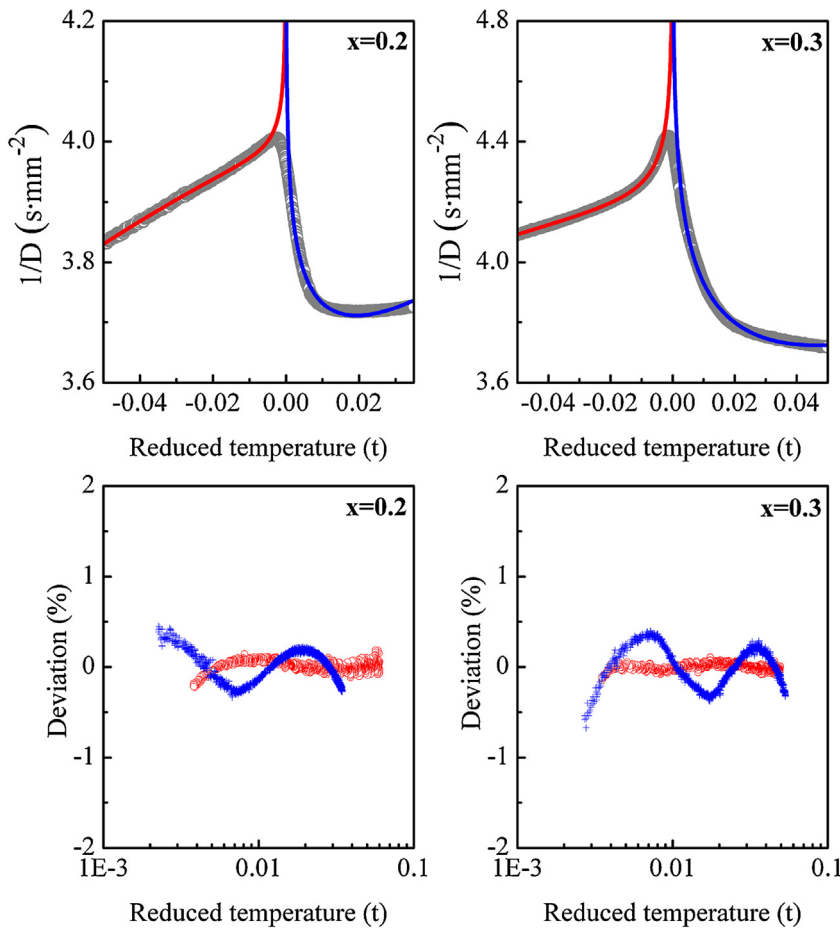


Fig. 7. $(Pb_xSn_{1-x})_2P_2S_6$ ($x=0.2, 0.3$). Above: Experimental data (circles) for the inverse of thermal diffusivity as a function of the reduced temperature $t=(T-T_C)/T_C$. The lines represent the fits to Eq. (9), fitting both branches at the same time. Below: Deviation plots corresponding to the fits shown above. Open circles are for $T < T_C$ and crosses for $T > T_C$.

means there is a clear change in the critical behaviour of the transition as Pb doping is increased.

Trying to elucidate that evolution, several different models have been checked applying them only to the paraelectric phase as it has been done before in $Sn_2P_2(Se_{x}S_{1-x})_6$, where there is a Lifshitz point at $x=0.28$ and a virtual tricritical point at $x \approx 0.6$. The presence of a Lifshitz point enhances the fluctuations in the order parameter with the consequence that the critical exponent will deviate from the mean-field values (α will change from 0 to $\alpha=1/4$ in the presence of short range interactions). But such fluctuations can be reduced in the case of ferroelectrics with strong dipolar interactions (it would lead to $\alpha=1/6$) or by the presence of a tricritical point. In the particular case of a tricritical Lifshitz point α should be 0.5 with small logarithmic corrections [4]. This last behaviour was suggested in reference [7] for $Sn_2P_2S_6$ but later discarded in [11] where it was shown that a combination of the fluctuation effects plus the contribution of defects had to be taken into account to correctly fit the experimental values; this mechanism was suggested by Isaverdiyev et al. [36–38]. As $(Pb_xSn_{1-x})_2P_2S_6$ with $x=0.1, 0.2$ do not differ much from $Sn_2P_2S_6$, those two last models have been tested for the fittings.

If we first take into account only first-order fluctuations, the fitting equation is

$$\frac{1}{D} = B_2 + C_2 t + A_2 |t|^{-\alpha} \quad (10)$$

where α should be 0.5. If we consider the possibility of the attenuation of fluctuations in the order parameter, we should introduce

a small logarithmic correction, whose effect would be to slightly reduce the value α in Eq. (10) from the exact 0.5 value:

$$\frac{1}{D} = B_3 + C_3 t + A_3 |t|^{-0.5} |\ln |t||^b \quad (11)$$

And if we consider the possible superposition of fluctuation effects and the contribution of defects the equation will be

$$\frac{1}{D} = B_4 + C_4 t + A_4 |t|^{-0.5} + F_4 |t|^{-1.5} \quad (12)$$

In the three cases we have the linear background plus the anomalous term(s). Starting with $x=0.1$, the fitting to Eq. (10) was not possible with $\alpha=0.5$. Indeed, the best fitting was obtained for $\alpha=0.66$ which does not make sense and which annuls the possibility of even testing Eq. (11). On the other hand, Eq. (12) gave quite a good fitting which is presented in Fig. 8, together with the deviation plot (the relevant information about the fittings is presented in Table 2). The quotient of the parameters F_4/A_4 is 2.4×10^{-4} indicating that the amplitude of the defects contribution to the anomalous term in Eq. (12) is smaller than the amplitude of the fluctuational one but, nevertheless, the defect term $F_4 |t|^{-1.5}$ dominates at temperatures close enough to the critical temperature. This result is analogous to the one found in [11] for $x=0$, which is not surprising as Pb has been introduced only in a 10% proportion. Turning our attention to $x=0.2$, the best fitting to Eq. (10) gives $\alpha=0.37$, which is too far away from 0.5. Essays to obtain a good fit using Eq. (11) were not successful with small b values, as theory indicates it should be. On the other hand, the use of Eq. (12) gave a rather good fitting, presented in Fig. 8 and Table 2.

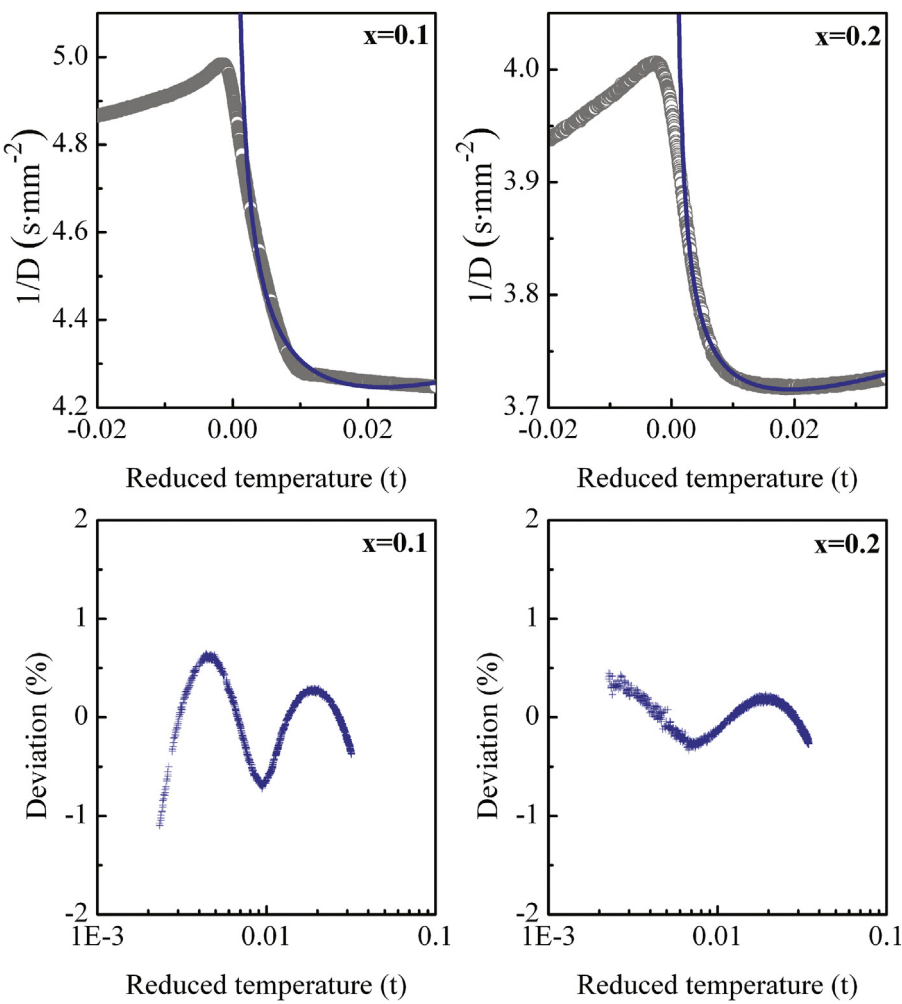


Fig. 8. $(\text{Pb}_x\text{Sn}_{1-x})_2\text{P}_2\text{S}_6$ ($x=0.1, 0.2$). Above: Experimental data (circles) for the inverse of thermal diffusivity as a function of the reduced temperature $t=(T-T_C)/T_C$. The lines represent the fits to Eq. (12), for the paraelectric phase. Below: Deviation plots corresponding to the fits shown above.

For the sake of completeness, even if a very good fitting has already been found for $x=0.3$ with Eq. (9), we have also checked these models using Eqs. (10)–(12). Eq. (10) gave quite a good fitting with $\alpha=-0.11$ (but worse than with Eq. (9)) and no fitting was possible neither with Eq. (11) nor with Eq. (12).

All these results give us a clear picture on how critical behaviour evolves as lead concentration is increased in $(\text{Pb}_x\text{Sn}_{1-x})_2\text{P}_2\text{S}_6$. In all cases the ferroelectric phase can be well described by the classical Landau model but this might be due to the fact that we can not get too close to the critical temperature on that side of the phase transition, so we can not see the influence of the possible fluctuations of the order parameter and their enhancement or attenuation by some other mechanisms.

The sample with $x=0.1$ has the same critical behaviour as $\text{Sn}_2\text{P}_2\text{S}_6$ where there are several competing mechanisms. On the one hand, the nearness to a Lifshitz point enhances the fluctuations of the order parameter while on the other one, the nearness to a tricritical point reduces them. Besides, point defects are responsible for inducing long-range perturbations of the order parameter. The combination of all of them is needed to take into account a clear deviation from a mean field model, which has been discarded by the appropriate fittings. As lead concentration is increased, a crossover to other universality classes starts, shown by the fact that the critical behaviour of the sample with $x=0.2$ can be explained by two models. In the first place, by a similar combination of mechanisms as for $x=0.1$ shown by the fitting of the paraelectric phase to Eq.

(12); secondly, the fitting to Eq. (9) using both the paraelectric and the ferroelectric phase gave a critical exponent $\alpha=-0.07$ close to the mean field model 0. At $x=0.3$, the fitting to Eq. (9) gave a very good fitting, with $\alpha=-0.04$, very close to the mean field model, while it was not possible to fit it to any model with had any relation to the nearness to Lifshitz or tricritical points or the contribution of point defects. To all effects, $x=0.3$ behaves as a common uniaxial ferroelectric. So we see a crossover from a non-mean field model to it. $x=0.2$ is an intermediate case in which the predominance of the long-range perturbations is not settled yet as it is in $x=0.3$.

5. Conclusions

The thermal diffusivity of the ferroelectric family $(\text{Pb}_x\text{Sn}_{1-x})_2\text{P}_2\text{S}_6$ ($x=0.1$ to 1) has been measured in a wide temperature range using an ac photopyroelectric calorimeter, confirming its thermal insulator behaviour and the predominant role of phonons as heat carriers. Thermal anisotropy has been confirmed in this monoclinic structure. The evolution of the critical behaviour of the paraelectric to ferroelectric transition has been studied, after having checked its continuous character. There is a crossover from a clear non-mean field model at $x=0.1$ (where the first-order fluctuations as well as the presence of defects must be taken into account) to a mean field one at $x=0.3$.

Acknowledgements

This work have been supported by Ministerio de Ciencia e Innovación with FEDER support (MAT2011-23811), Gobierno Vasco (IT619-13), and UPV/EHU (UFI11/55). V. Shvalya thanks the Erasmus Mundus programme “ACTIVE” for his grant.

Appendix A. Supplementary data

Supplementary data associated with this article can be found, in the online version, at <http://dx.doi.org/10.1016/j.tca.2015.08.031>.

References

- [1] A.A. Grabar, M. Jazbinsek, A.N. Shumelyuk, Yu.M. Vysochanskii, G. Montemezzani, P. Günter, Photorefractive effects in $\text{Sn}_2\text{P}_2\text{S}_6$, in: P. Günter, J.P. Huignard (Eds.), Photorefractive Materials and Their Applications II, Springer Series in Optical Science, 2007.
- [2] O. Mys, I. Martynyuk-Lototska, A.M. Kostruba, A. Grabar, R. Vlokh, Ukr. J. Phys. Opt. 13 (2012) 177.
- [3] Yu.M. Vysochanskii, T. Janssen, R. Currat, R. Folk, J. Banys, J. Grigas, V. Samulionis, Phase Transitions in Ferroelectric Phosphorous Chalcogenide Crystals, Vilnius University Publishing House, 2006.
- [4] R. Folk, G. Moser, Phys. Rev. B 47 (1993) 13992.
- [5] B.A. Strukov, E.P. Ragula, S.V. Arkhangelskaya, I.V. Shnaidstein, Phys. Solid State 40 (1998) 94.
- [6] R. Folk, G. Moser, J. Phys. A: Math. Gen. 39 (2006) R207.
- [7] Yu.M. Vysochanskii, V.V. Mitrovicij, A.A. Grabar, S.I. Perechinskii, S.F. Motrja, J. Kroupa, Ferroelectrics 237 (2000) 193.
- [8] Yu.M. Vysochanskii, S.I. Perechinskii, V.M. Rizak, I.M. Rizak, Ferroelectrics 143 (1993) 59.
- [9] Yu.M. Vysochanskii, A.A. Molnar, A.A. Gorvat, Yu.S. Nakonechnii, Ferroelectrics 169 (1995) 141.
- [10] V. Samulionis, J. Banys, Yu.M. Vysochanskii, A.A. Grabar, Phys. Status Solidi (b) 215 (1999) 1151.
- [11] A. Oleaga, A. Salazar, M. Massot, Yu. Vysochanskii, Thermochim. Acta 459 (2007) 73.
- [12] A. Say, O. Mys, D. Adamenko, A. Grabar, Yu. Vysochanskii, A. Kityk, R. Vlokh, Phase Trans. 83 (2010) 123.
- [13] A. Say, O. Mys, A. Grabar, Yu. Vysochanskii, R. Vlokh, Phase Trans. 82 (2009) 531.
- [14] A. Oleaga, A. Salazar, A.A. Kohutych, Yu.M. Vysochanskii, J. Phys.: Condens. Matter 23 (2011) 025902.
- [15] R. Folk, Phase Trans. 67 (1999) 645.
- [16] K. Moriya, K. Iwauchi, M. Ushida, A. Nakagawa, K. Watanabe, S. Yano, S. Motojima, Y. Akagi, J. Phys. Soc. Jpn. 64 (1995) 1775.
- [17] M. Marinelli, F. Mercuri, U. Zammit, R. Pizzoferrato, F. Scudieri, D. Dadarlat, Phys. Rev. B 49 (1994) 9523.
- [18] A. Salazar, M. Massot, A. Oleaga, A. Pawlak, W. Schranz, Phys. Rev. B 75 (2007) 224428.
- [19] A. Oleaga, A. Salazar, D. Prabhakaran, A.T. Boothroyd, Phys. Rev. B 70 (2004) 184402.
- [20] A. Oleaga, A. Salazar, Yu.M. Bunkov, J. Phys.: Condens. Matter 26 (2014) 096001.
- [21] A. Oleaga, A. Salazar, M. Massot, A. Molak, M. Koralewski, Ferroelectrics 369 (2008) 76.
- [22] F. Mercuri, U. Zammit, M. Marinelli, Phys. Rev. E 57 (1998) 596.
- [23] U. Zammit, M. Marinelli, F. Mercuri, S. Paoloni, F. Scudieri, Rev. Sci. Instrum. 82 (2011) 121101.
- [24] J. Grigas, E. Tali, V. Lazauskas, Yu.M. Vysochanskii, R. Yevych, M. Adamiec, V. Nelkinas, Lith. J. Phys. 48 (2008) 145.
- [25] K. Moriya, T. Yamada, K. Sakai, S. Yano, S. Baluja, T. Matsuo, I. Pritz, Y.M. Vysochanskii, J. Therm. Anal. Calorim. 70 (2002) 321.
- [26] M. Marinelli, U. Zammit, F. Mercuri, R. Pizzoferrato, J. Appl. Phys. 72 (1992) 1096.
- [27] M. Chirtoc, D. Dadarlat, D. Bicanic, J.S. Antoniou, M. Egée, in: A. Mandelis, P. Hess (Eds.), Progress in Photochemical and Photoacoustic Science and Technology, vol. 3, SPIE, Bellingham, Washington, 1997.
- [28] S. Delenclos, M. Chirtoc, A. Hadj Sahraoui, C. Kolinsky, J.M. Buisine, Rev. Sci. Instrum. 73 (2002) 2773.
- [29] A. Salazar, Rev. Sci. Instrum. 74 (2003) 825.
- [30] V.M. Rizak, K. Al-Shoufi, I.M. Rizak, Yu. Vysochanskii, V.Yu. Slivka, Ferroelectrics 192 (1999) 177.
- [31] M.M. Khoma, A.A. Molnar, Yu. Vysochanskii, J. Phys. Stud. 2 (1998) 524.
- [32] Yu. Vysochanskii, V.M. Rizak, I.M. Rizak, M.I. Gurzan, V.Yu. Slivka, Ukr. Phys. J. 37 (1992) 1745.
- [33] A. Kornblit, G. Ahlers, Phys. Rev. B 11 (1975) 2678.
- [34] G. Ahlers, A. Kornblit, Phys. Rev. B 12 (1975) 1938.
- [35] A. Oleaga, A. Salazar, D. Prabhakaran, J.G. Cheng, J.S. Zhou, Phys. Rev. B 85 (2012) 184425.
- [36] A.A. Isaverdiyev, N.I. Lebedev, A.P. Levanyuk, A.S. Sigov, Fiz. Tverd. Tela 31 (1989) 272.
- [37] A.A. Isaverdiyev, N.I. Lebedev, A.P. Levanyuk, A.S. Sigov, Ferroelectrics 117 (1991) 135.
- [38] A.A. Isaverdiyev, A.P. Levanyuk, A.S. Sigov, Ferroelectrics 117 (1991) 141.